IEEE Photonics Journal
An IEEE Photonics Society Publication

Open Access

Mode Couplers and Converters Based on Dual-Core Hollow-Core Photonic Bandgap Fiber

Volume 10, Number 2, April 2018

Simeng Han
Zhi Wang
Yange Liu
Hongye Li
Hu Liang
Zhenhong Wang

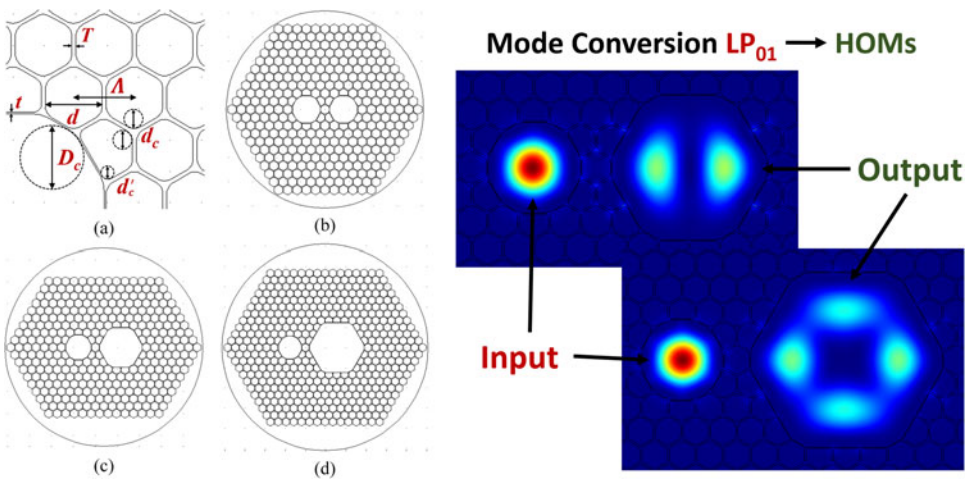

DOI: 10.1109/JPHOT.2018.2810059
1943-0655 © 2018 IEEE

IEEE photonics SOCIETY

IEEE

Mode Couplers and Converters Based on Dual-Core Hollow-Core Photonic Bandgap Fiber

Simeng Han, Zhi Wang, Yange Liu, Hongye Li, Hu Liang, and Zhenhong Wang

Tianjin Key Laboratory of Optoelectronic Sensor and Sensing Network Technology, and Institute of Modern Optics, Nankai University, Tianjin 300071, China

DOI:10.1109/JPHOT.2018.2810059
1943-0655 © 2018 IEEE. Translations and content mining are permitted for academic research only. Personal use is also permitted, but republication/redistribution requires IEEE permission. See http://www.ieee.org/publications_standards/publications/rights/index.html for more information.

Manuscript received January 23, 2018; revised February 18, 2018; accepted February 23, 2018. Date of publication February 28, 2018; date of current version March 23, 2018. This work was supported in part by the National Natural Science Foundation of China under Grants 61322510, 61640408, and 61775107, and in part by Tianjin Natural Science Foundation under Grant 16JCZDJC31000, China.
Corresponding author: Zhi Wang (e-mail: zhiwang@nankai.edu.cn).

Abstract: We propose mode couplers and converters based on dual-core hollow-core photonic bandgap fiber (HC-PBGF) structures, which might be potential solutions for integrated all-fiber multiplexers or demultiplexers of a mode-division multiplexed (MDM) transmission system using HC-PBGFs. Coupling properties of LP_{01} and LP_{11} mode in the mode coupler are investigated and applied to mode separators and polarization separators. Mode transition from LP_{01} to LP_{11} and LP_{21} mode are demonstrated in the mode converter whose smaller core is expected as input end and matched with single-mode fiber. The coupling between fundamental mode and high-order modes is accomplished through the resonant effect, which is fulfilled by modifying the structure parameter of the smaller core. Such mode converters based on dual-core HC-PBGF could be a promising substitute for the free-space coupling device, which is costly and not suitable for integration design in MDM systems and other hollow-core fiber experiments and applications.

Index Terms: Fiber communication, fiber couplers, hollow-core photonic bandgap fiber, mode conversion.

1. Introduction

Since the initially conceptual and practical demonstrations in 1990s, hollow-core photonic bandgap fibers (HC-PBGFs) have attracted enormous attention owing to their intriguing properties that are absent in the conventional solid fiber [1]. Air guidance in HC-PBGF provides it with low latency [2], which is of great interest for various time-sensitive applications including intra- and inter-data center interconnection, high performance computing, high energy physics experiment, and data networks for the financial sector. In addition, the ultralow nonlinearity, low thermal sensitivity [3], broad bandwidth along with the potential for ultralow transmission loss and intrinsic multimode nature have made HC-PBGF a promising candidate in the next-generation high speed and large-capacity optical transmission systems using mode-division multiplexed (MDM) technology [4], which can overcome the "capacity crunch" of current single-mode fiber (SMF) networks imposed by the nonlinear effect [5], [6]. Recently, massive experimental low latency, high capacity transmission systems based on HC-PBGF have been demonstrated both in the conventional C-band [2], [4], [7], [8] and a new spectral band for telecommunications around 2 μm [9]–[11]. The shifting of the

transmission band was introduced on account of the lowest predicted loss window of HC-PBGF lying around 2 μm [12], [13], within the working wavelength of Thulium-doped fiber amplifiers (TDFAs) [14], [15].

One of the most fundamental and essential issues in MDM transmission systems and other fiber experiments and applications is the mode multiplexer and de-multiplexer, the devices which realize mode conversion. Currently, multiplexers and de-multiplexers in HC-PBGF transmission systems commonly adopt free space coupling device, which reduce the integrity and flexibility of the system. Compared with spatial devices, an all-fiber structure is more convenient and compact. Fiber couplers utilizing resonant effect are widely investigated and applied. Mode selective couplers with conventional silica glass fibers or waveguides have been demonstrated and fabricated maturely in simulations and experiments [16], [17], and perform well as mode converters in applications on MDM transmission systems [18]–[20] and others [21]. Mode couplers or multiplexers with solid-core photonic crystal fiber structures have also been proposed and researched [22], yet fiber couplers based on hollow-core fibers are less investigated. HC-PBGFs with larger core (19 or 37 cells) are intensively employed in MDM transmission owing to their lower loss and intrinsic multi-mode nature [4]. However, the core of such fiber is much larger than that of SMF, which makes it less compatible with current SMF transmission systems. As far as we are concerned, an all-fiber structure whose input end is commensurate with core size of SMF for mode-multiplexing in hollow-core fiber might be a more convenient and economical approach. Unlike the conventional fiber and solid core photonic crystal fiber whose mode properties can be varied through being filled with liquid and doping, the design of HC-PBGF for realizing the mode match for resonant condition is more difficult and limited.

In this letter, we propose potential dual-core HC-PBGF structures as solutions for all-fiber hollow-core fiber multiplexers and de-multiplexers. Mode couplers and mode converters based on symmetric and asymmetric dual-core HC-PBGF structures are demonstrated. Mode coupling of both LP_{01} and LP_{11} mode are analyzed in a symmetric 7-cell dual-core HC-PBGF coupler in detail, which can be used as polarization and mode separators. In the more interesting part, mode conversion from LP_{01} to LP_{11} and from LP_{01} to LP_{21} are demonstrated in 7, 19-cell dual-core HC-PBGF and 7, 37-cell dual-core HC-PBGF, respectively. The core diameter of the smaller 7-cell core in each structure is comparable with the core diameter of SMF. The resonant condition of modes in adjacent cores is realized by modifying the core parameter of the 7-cell core. Such structures are compatible with the current fiber communication systems, and provide a novel and potential approach to accomplish mode-multiplexing in HC-PBGF-based MDM transmission systems in an integration all-fiber structure.

2. Structures and Method

Fig. 1(a) shows the cross-section and the defined structure parameters in the vicinity of the 7-cell core. The structure of photonic crystal in the cladding is formed by a triangular arrangement of hexagonal air holes with the lattice constant $\Lambda = 3.86\,\mu$m, which is matched with the operating wavelength of TDFA. The air core is introduced into the HC-PBGF by removing 7 air holes from the cladding structure. The diameter of cladding air hole is $d = 3.61\,\mu$m and the corners are rounded with circles of diameter $d_c = 0.44\,\Lambda$ and $d_c' = 0.25\,\Lambda$. The thickness of silica in cladding is $T = 0.25\,\mu$m and the thickness of silica ring around the air core is $t = 0.5\,$T, which assure that the fiber is less affected by surface modes (SMs) [23], [24]. The curvature of the round corner of air core D_c is a crucial parameter. Effective refractive index (n_{eff}) of LP_{01} mode in this core can be varied by modifying D_c, which can achieve the match of n_{eff} between different modes in the asymmetric structures. Cross-sections of three different dual-core HC-PBGFs are shown in Fig. 1(b)–(d), and the length between the centers of the two cores of each structure is 4 Λ, 5 Λ, and 6 Λ. All the structures are free from surface modes (SMs). The refractive index of air holes and background silica are 1 and 1.4384, respectively. The material dispersion is neglected since the light propagates mainly in air.

The mode coupling of the dual-core HC-PBGF is investigated by a commercial full-vector finite-element method software COMSOL. We obtain the effective index value and the field distribution

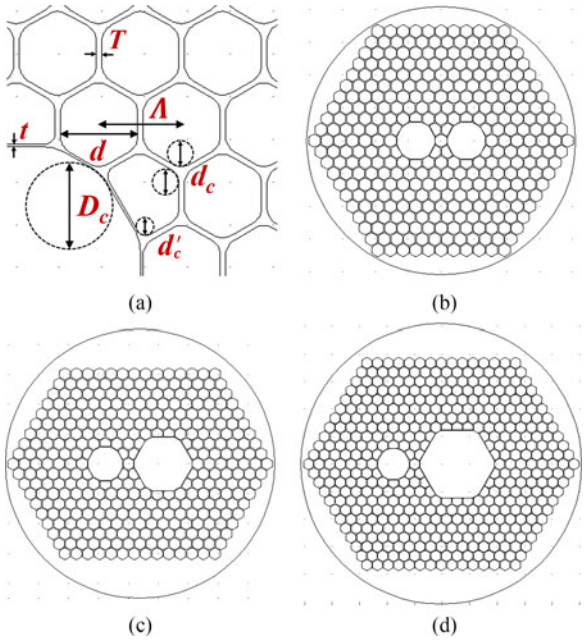

Fig. 1. (a) Detailed parameters of the simulation structure. (b), (c), (d) Cross-section of symmetric 7-cell dual-core HC-PBGF and asymmetric 7, 19-cell, 7, 37-cell dual-core HC-PBGF.

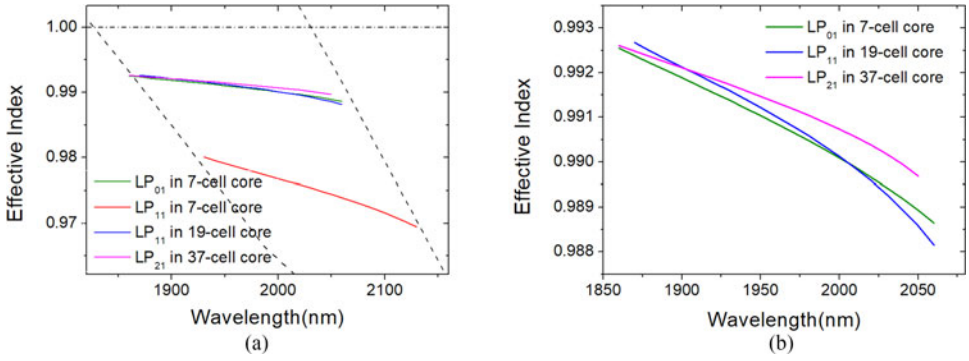

Fig. 2. (a) n_{eff} of different guided modes as well as the photonic bandgap (PBG) edges as a function of wavelength. (b) The enlarged view of the top group modes.

of the eigenmodes. Only half of the structure is considered in the simulation, which is allowed by the geometrical symmetry of our structure.

The coupling properties of dual-core HC-PBGF are mainly characterized by coupling length L_c, which is defined as

$$L_c = \lambda/2 \left| n_{eff,e,i} - n_{eff,o,i} \right|, i = x, y \tag{1}$$

where $n_{eff,e,i}$ and $n_{eff,o,i}$ are the effective index of the i-polarized even and odd supermodes, respectively. λ is the vacuum wavelength.

3. Simulation Results

To begin with, we investigate the properties of guided modes in the single-core PBGFs with different core dimensions. Fig. 2(a) shows the n_{eff} of different guided modes as well as the photonic bandgap

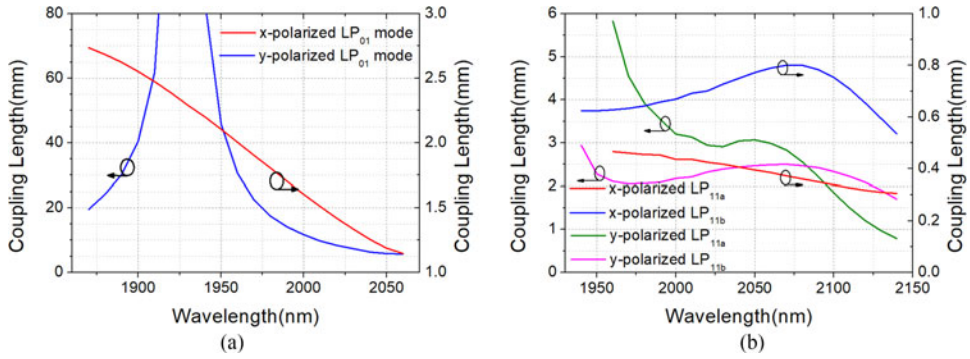

Fig. 3. Coupling length of (a) LP_{01} mode and (b) LP_{11} mode.

(PBG) edges as a function of wavelength. We use circular air holes instead of hexagonal ones in a plane wave expansion (PWE) method software MPB to calculate the PBG approximately so that we can find the deviation between the n_{eff} curves and PBG edges. Fig. 2(b) is the enlarged view of the top mode group. We can point out that the n_{eff} values of LP_{01} mode in 7-cell core and HOMs in larger cores are comparative over the approximate 200 nm bandwidth. However, since the dimensions of the two cores are diverse, the dispersion curves of modes in different cores are not identical. The coupling between the two cores with different dimensions occurs through the resonant effect between the two modes. Furthermore, a much better coupling phenomenon can be achieved at the specific wavelength only if the n_{eff} values of the two modes are completely equal. As exhibited in Fig. 2(b), the differential of the n_{eff} curve slopes between LP_{01} mode and HOMs promise the intersection of the two curves at the particular wavelength through appropriate design of the structures.

3.1 Mode Couplers

The coupling properties of dual-core PBGF are first researched in a symmetric structure, which has two 7-cell cores. The x-polarized and y-polarized LP_{11} modes are no longer degenerated since the circular symmetry is destroyed drastically by the introduction of the two cores. So, we believe that modes with different polarizations have different coupling properties. Fig. 3(a) shows the coupling length of LP_{01} mode as a function of wavelength. We can find a decoupling phenomenon in the y-polarized mode, which is coincident with ref. [25]. The discrepancy of coupling properties between different polarizations is remarkable. Furthermore, such a discrepancy is found in LP_{11} mode. Fig. 3(b) shows the coupling length of LP_{11a} and LP_{11b} mode as a function of wavelength. The variation of coupling length of each mode is complicated, while the distinction between the two polarizations is obvious. From our perspective, properties such as decoupling and polarization dependence can be attributed to the effect of SMs, that SMs have different influence on x- and y-polarized supermodes.

According to the aforementioned properties, we can accomplish the design of mode separators and polarization separators at the particular wavelength by employing such dual-core HC-PBGFs with appropriate fiber length. We demonstrate some fundamental design examples in Fig. 4. Fig. 4(a), (b), (c), and (d) show the separation of different polarizations of LP_{01} mode, different polarizations of LP_{11a} mode, different polarizations of LP_{11b} mode, and separation of x-polarized LP_{01} and LP_{11a} mode, respectively. The input and output ports are marked in each figure. The arrows represent the polarizations. Both modes distribute in the same core at the input end, while two modes separate from each other and distribute in different cores after propagating through the fiber. Owing to the scalability of PBG, we can fulfill such mode separators in any wavelength by modifying the dual-core PBGF in proportion.

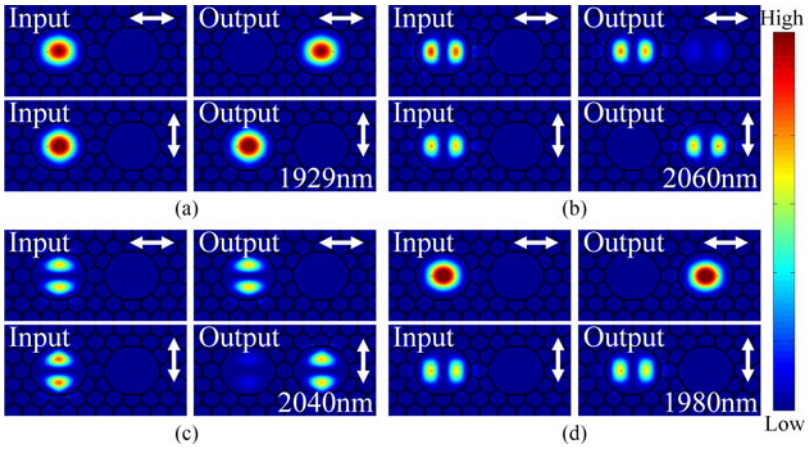

Fig. 4. Separations between different polarized modes and different modes. (a) Mode separation of different polarization LP_{01} mode in 1929 nm. (b) Mode separation of different polarization LP_{11a} mode in 2060 nm. (c) Mode separation of different polarization LP_{11b} mode in 2040 nm. (d) Mode separation of x-polarized LP_{01} and LP_{11a} mode in 1980 nm. In each circumstance, we input two modes in the same core, while two modes distribute in different cores in the output end. The arrows represent the polarizations.

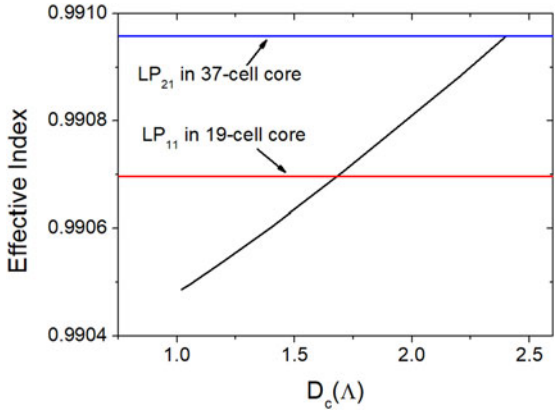

Fig. 5. Black solid curve: n_{eff} value of LP_{01} mode as a function of D_c at 1980 nm. Red and blue solid lines: n_{eff} value of LP_{11} and LP_{21} modes.

3.2 Mode Converters

Unlike the symmetric structure, dual-core PBGF with a different core dimension experienced a distinct coupling process. As we mentioned earlier, three mode's n_{eff} are comparative and three curves experience intersection over the 200 nm bandwidth. The coupling between the two cores occurs through the resonant effect between the two modes. We can move the intersection point to the needed wavelength, which means we can attain the best coupling phenomenon at the specific wavelength. To fulfill the resonance condition, we should match the n_{eff} values between LP_{01} mode and HOMs. For such structures, the larger core is the expected output end while the smaller 7-cell core is proposed to be the input end and matched with SMF. Hence, modifying the parameter of the 7-cell core is a more appropriate and convenient approach to accomplish the match of n_{eff}. As we mentioned earlier, n_{eff} of LP_{01} mode in the 7-cell core can be varied by altering the value of D_c. Fig. 5 shows the n_{eff} value of x-polarized LP_{01} mode as a function of D_c at the working wavelength with a black solid curve. The linear increase in the n_{eff} value of LP_{01} mode with the augment of D_c can be attributed to the impact of SMs. Since the modifying of D_c changes the silica region

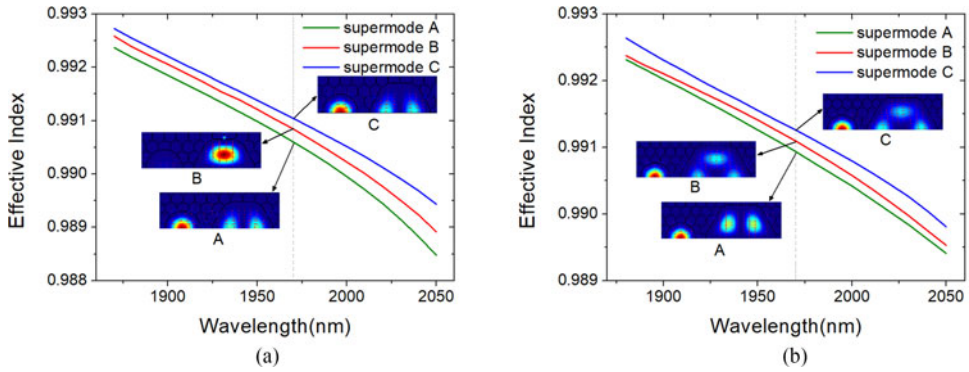

Fig. 6. n_{eff} curves of supermodes and distribution of supermodes in (a) 7, 19-cell structure and (b) 7, 37-cell structure.

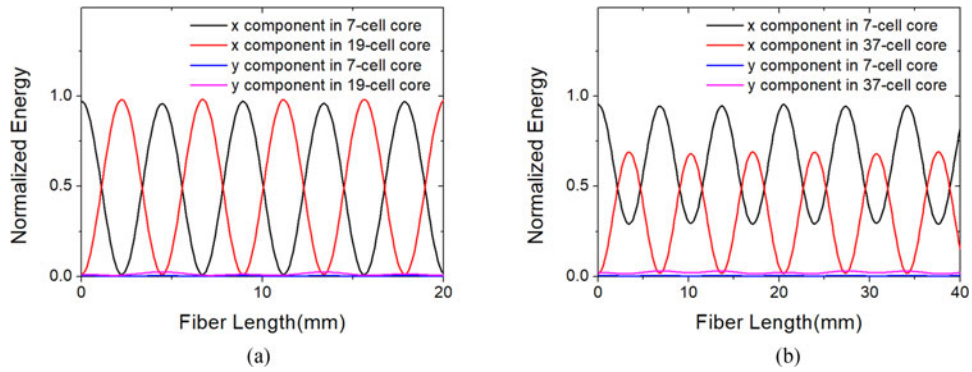

Fig. 7. Mode conversion dominated by x-polarized LP_{11a} (LP_{21a}) mode. Normalized energy as a function of fiber length (a) in 7, 19-cell structure and (b) in 7, 37-cell structure.

around the core where SMs mainly locate in, the n_{eff} curves of surface modes are varied. SMs can affect the guiding mode in the core through avoided crossing effect though SMs are not supported inside the PBG, and the position of the avoided crossing point shifts on account of the variation of SMs. Consequently, the n_{eff} curve of guiding mode is regulated.

The n_{eff} values of LP_{11} mode in 19-cell core and LP_{21} mode in 37-cell core at 1970 nm are also shown in Fig. 5 with red solid line and blue solid line, respectively. Eventually, we set $D_c = 1.7\,\Lambda$ in the 7, 19-cell structure and $D_c = 2.4\,\Lambda$ in the 7, 37-cell structure. The resonant condition we discussed here is applied to x-polarized LP_{01} mode. Fig. 6(a) and (b) show the effective index values of supermodes of 7, 19-cell structure and 7, 37-cell structure over 200 nm, respectively. We also exhibit the distribution of supermodes in the two structures at 1970 nm. For each structure, the coupling process between LP_{01} mode and LP_{11} (LP_{21}) mode is characterized by three supermodes. The n_{eff} curves of LP_{01} mode in 7-cell core, x-polarized LP_{11a} (LP_{21a}) mode, and y-polarized LP_{11b} (LP_{21b}) mode in 19-cell core transform to curves of supermodes A, B and C through avoided crossing effect. The coupling between LP_{01} mode and x-polarized LP_{11a} (LP_{21a}) is relatively dominant over the 200 nm bandwidth, while conversion from LP_{01} mode to y-polarized is not always as strong as the former, which is dependent on the distribution of supermode B. For example, at 1970 nm for the two structures, the different distributions of supermode B in 7-cell core determine that the coupling between LP_{01} to y-polarized HOM is strong in 7, 37-cell structure and weak in 7, 19-cell structure.

Fig. 7(a) and (b) show the normalized energy of different polarized components of two structures as a function of propagating fiber length. We can easily find out that the x-component in 7-cell and 37-cell core represent x-polarized LP_{01} and LP_{11a} (LP_{21a}) mode, while the y-component in

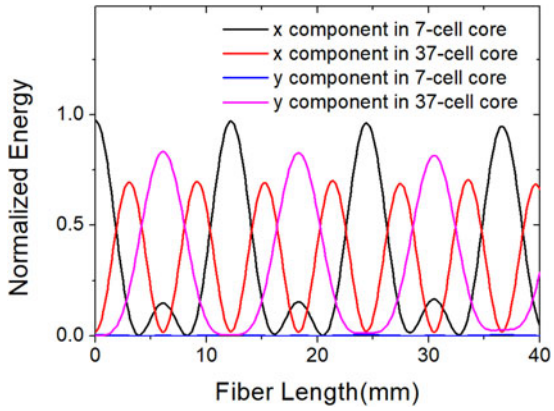

Fig. 8. Mode conversion into both x-polarized LP_{21a} and y-polarized LP_{21b} in 7, 37-cell structure.

37-cell core represent y-polarized LP_{11b} (LP_{21b}) mode. In these two processes, mode conversion from x-polarized LP_{01} mode to x-polarized LP_{11a} and LP_{21a} is dominant. Transition of energy to y-polarized LP_{11b} and LP_{21b} mode exists, yet it is weak and negligible. But at some wavelength, the energy coupled into y-polarized HOMs is comparable with that of x-polarized HOMs, which cannot be ignored. Fig. 8 shows an example of such a circumstance in 7, 37-cell structure. It is intriguing that both x-polarized LP_{11a} mode and y-polarized LP_{11b} mode participate in the coupling process evidently, whereas the oscillating energy transition curves of two modes along the propagating fiber length are disparate. The oscillating period or the so-called coupling length of y-polarized LP_{21b} mode is roughly double that of x-polarized LP_{11a} mode. With such a property, we can selectively design a structure in which energy is transferred into *i*-polarized HOM alone.

The conversion from y-polarized LP_{01} mode to HOMs is similar; consequently, we will not go into details.

4. Conclusion

In conclusion, we numerically studied the coupling properties of the dual-core PBGF structures we demonstrated, and proposed the mode coupler and mode converter based on such structures. Coupling process of both LP_{01} and LP_{11} modes were investigated in the mode coupler. The polarization dependence of mode coupling was utilized in mode separators and polarization separators in any wavelength under specific parameters. For the mode converter, we reported the transition from LP_{01} mode in a smaller core to HOMs (LP_{11}, LP_{21}) in a larger core, which was realized by modifying the parameter of the 7-cell core. The mode conversion in such a structure provides a novel and potential approach to achieve mode-multiplexing in HC-PBGF MDM systems.

Compared with the work presented before [25], the dual-core PBGF structures we proposed here expand the decoupling phenomenon or the polarization dependence phenomenon to LP_{11} mode and realized mode separators. What is more, unlike the previous researches on the conventional fiber couplers [16], [17] or solid-core PBGF converters or multiplexers [22], [26], we firstly demonstrated mode conversion in hollow-core PBGF structures whose input cores are comparable with cores of SMF. Except for being a convenient and compact substitute of spatial device, the structures we raised here have several advantages over current mode-multiplexing device, including expanding the resonant couplers to the hollow-core fiber field, compatibility with SMF, and no need of complicated control system compared with photonic lantern. Over the past few years, long-haul and low loss HC-PBGFs have been manufactured experimentally [8], [9]. We believe the fabrication of our mode couplers and converters based on dual-core HC-PBGF structure can be realized under appropriate methods and technology.

References

[1] R. F. Cregan, B. J. Mangan, J. C. Knight, T. A. Birks, P. J. Roberts, and D. C. Allan, "Single-mode photonic band gap guidance of light in air," *Science*, vol. 285, pp. 1537–1539, 1999.

[2] F. Poletti *et al.*, "Towards high-capacity fibre-optic communications at the speed of light in vacuum," *Nature Photon.*, vol. 7, pp. 279–284, 2013.

[3] D. J. Richardson, E. N. Fokoua, F. Poletti, M. N. Petrovich, R. Slavík, and T. Bradley, "How to make the propagation time through an optical fiber fully insensitive to temperature variations," *Optica*, vol. 4, pp. 659–668, 2017.

[4] V. A. J. M. Sleiffer *et al.*, "High capacity mode-division multiplexed optical transmission in a novel 37-cell hollow-core photonic bandgap fiber," *J. Lightw. Technol.*, vol. 32, no. 4, pp. 854–863, Feb. 2014.

[5] D. J. Richardson, J. M. Fini, and L. E. Nelson, "Space-division multiplexing in optical fibres," *Nature Photon.*, vol. 7, pp. 354–362, 2013.

[6] E. Temprana *et al.*, "APPLIED OPTICS. Overcoming Kerr-induced capacity limit in optical fiber transmission," *Science*, vol. 348, pp. 1445–1448, 2015.

[7] B. J. Mangan *et al.*, "First demonstration of hollow-core fiber for intra data center low latency connectivity with a commercial 100 Gb/s Interface," in *Proc. Opt. Fiber Commun. Conf. Exhib.*, 2015, pp. 1–3.

[8] Y. Chen, Z. Liu, S. R. Sandoghchi, and G. Jasion, "Demonstration of an 11 km hollow core photonic bandgap fiber for broadband low-latency data transmission," in *Proc. Opt. Fiber Commun. Conf. Exhib.*, 2015, pp. 1–3.

[9] Y. Chen *et al.*, "Multi-kilometer long, longitudinally uniform hollow core photonic bandgap fibers for broadband low latency data transmission," *J. Lightw. Technol.*, vol. 34, no. 1, pp. 104–113, Jan. 2016.

[10] H. Zhang, Z. Li, N. Kavanagh, and J. Zhao, "81 Gb/s WDM transmission at 2 μm over 1.15 km of low-loss hollow core photonic bandgap fiber," in *Proc. Eur. Conf. Opt. Commun.*, 2014, pp. 1–3.

[11] H. Zhang *et al.*, "100 Gbit/s WDM transmission at 2 μm: transmission studies in both low-loss hollow core photonic bandgap fiber and solid core fiber," *Opt. Exp.*, vol. 23, pp. 4946–4951, 2015.

[12] P. Roberts *et al.*, "Ultimate low loss of hollow-core photonic crystal fibres," *Opt. Exp.*, vol. 13, pp. 236–244, 2005.

[13] J. K. Lyngsø, B. J. Mangan, C. Jakobsen, and P. J. Roberts, "7-cell core hollow-core photonic crystal fibers with low loss in the spectral region around 2 microm," *Opt. Exp.*, vol. 17, pp. 23468–23473, 2009.

[14] Z. Li *et al.*, "Diode-pumped wideband thulium-doped fiber amplifiers for optical communications in the 1800–2050 nm window," *Opt. Exp.*, vol. 21, pp. 26450–26455, 2013.

[15] M. N. Petrovich *et al.*, "Demonstration of amplified data transmission at 2 μm in a low-loss wide bandwidth hollow core photonic bandgap fiber," *Opt. Exp.*, vol. 21, pp. 28559–28569, 2013.

[16] R. Ismaeel, T. Lee, B. Oduro, Y. Jung, and G. Brambilla, "All-fiber fused directional coupler for highly efficient spatial mode conversion," *Opt. Exp.*, vol. 22, pp. 11610–11619, 2014.

[17] R. Ismaeel and G. Brambilla, "Removing the directional degeneracy of LP_{11} mode in a fused-type mode selective coupler," *J. Lightw. Technol.*, vol. 34, no. 4, pp. 1242–1246, Feb. 2016.

[18] N. Hanzawa *et al.*, "Two-mode PLC-based mode multi/demultiplexer for mode and wavelength division multiplexed transmission," *Opt. Exp.*, vol. 21, pp. 25752–25760, 2013.

[19] S. H. Chang *et al.*, "Mode division multiplexed optical transmission enabled by all-fiber mode multiplexer," *Opt. Exp.*, vol. 22, pp. 14229–14236, 2014.

[20] K. Igarashi, K. J. Park, T. Tsuritani, I. Morita, and B. Y. Kim, "All-fiber-based selective mode multiplexer and demultiplexer for weakly-coupled mode-division multiplexed systems," *Opt. Commun.*, vol. 408, pp. 58–62, 2017.

[21] Y. Shen *et al.*, "Switchable narrow linewidth fiber laser with LP_{11} transverse mode output," *Opt. Laser Technol.*, vol. 98, pp. 1–6, 2018.

[22] S. Yerolatsitis and T. A. Birks, "Three-mode multiplexer in photonic crystal fibre," in *Proc. Eur. Conf. Exhib. Opt. Commun.*, 2013, pp. 1–3.

[23] J. West, C. Smith, N. Borrelli, D. Allan, and K. Koch, "Surface modes in air-core photonic band-gap fibers," *Opt. Exp.*, vol. 12, pp. 1485–1496, 2004.

[24] R. Amezcua-Correa *et al.*, "Control of surface modes in low loss hollow-core photonic bandgap fibers," *Opt. Exp.*, vol. 16, pp. 1142–1149, 2008.

[25] Z. Wang *et al.*, "Coupling and decoupling of dual-core photonic bandgap fibers," *Opt. Lett.*, vol. 30, pp. 2542–2544, 2005.

[26] M. Y. Lan, S. Y. Cai, S. Yu, W. Y. Gu, Y. J. Zhang, and Y. Wang, "Mode converter based on dual-core all-solid photonic bandgap fiber," *Photon. Res.*, vol. 3, pp. 220–223, 2015.